Predicting oral absorption of fenofibrate in lipid-based drug delivery systems by combining *in vitro* lipolysis with the mucus-PVPA permeability model

Margherita Falavigna[a], Mette Klitgaard[b], Ragna Berthelsen[b], Anette Müllertz[b], Gøril Eide Flaten[a*]

[a] Drug Transport and Delivery Research Group, Department of Pharmacy, UiT The Arctic University of Norway, Universitetsveien 57, 9037 Tromsø, Norway. margherita.falavigna@uit.no; goril.flaten@uit.no.

[b] Physiological Pharmaceutics, Department of Pharmacy, University of Copenhagen, Universitetsparken 2-4, 2100, Copenhagen, Denmark. mette.klitgaard@sund.ku.dk; ragna.berthelsen@sund.ku.dk; anette.mullertz@sund.ku.dk.

[*]Corresponding author

Abstract

The aim of this work was to develop a new *in vitro* lipolysis-permeation model to predict the *in vivo* absorption of fenofibrate in self-nanoemulsifying drug delivery systems (SNEDDSs). More specifically, the *in vitro* intestinal lipolysis model was combined with the mucus-PVPA (Phospholipid Vesicle-based Permeation Assay) *in vitro* permeability model. Biosimilar mucus (BM) was added to the surface of the PVPA barriers to closer simulate the intestinal mucosa. SNEDDSs for which pharmacokinetic data after oral dosing to rats was available in the literature were prepared, and the ability of the SNEDDSs to maintain fenofibrate solubilized during *in vitro* lipolysis was determined, followed by the assessment of drug permeation across the mucus-PVPA barriers. The amount of drug solubilized over time during *in vitro* lipolysis did not correlate with the AUC (area under the curve) of the plasma drug concentration curve. However, the AUC of the drug permeated after *in vitro* lipolysis displayed a good correlation with the *in vivo* AUC ($R^2 > 0.9$). Thus, it was concluded that the *in vitro* lipolysis–mucus-PVPA permeation model, simulating the physiological digestion and absorption processes, was able to predict *in vivo* absorption data, exhibiting great potential for further prediction of *in vivo* performance of SNEDDSs.

Keywords: Gastrointestinal tract; *In Vitro/In Vivo* (IVIVC) Correlation; *In vitro* model; Lipid-based formulation; Oral drug delivery; Permeability; Poorly water-soluble drug; Precipitation; Self-emulsifying.

1. Introduction

In the past decades, lipid-based drug delivery systems (LbDDSs) have attracted increasing attention due to their ability to improve the bioavailability of poorly water-soluble drugs[1] *via* solubilization enhancement, supersaturation[2, 3], permeation enhancement and lymphatic transport[4]. Among LbDDSs, self-nanoemulsifying drug delivery systems (SNEDDSs; mixture of oil, surfactant, co-surfactant and co-solvent) have especially been studied because of their ability to spontaneously form nanoemulsions after dispersion in an aqueous environment. Once entered into the gastrointestinal (GI) tract, these formulations are dispersed in the gastric and intestinal fluids and are concomitantly affected by digestive enzymes. These physiological processes result in the formation of a wide range of colloidal structures able to affect the solubilization of the administered drug, and thus impacting its absorption[5]. Although several studies have been carried out regarding the potential of LbDDSs as oral drug delivery systems[3, 6-8] and several LbDDSs have reached the market[9], the development of an optimal LbDDS is still regarded as a challenging process[1]. The main reason for this is that numerous excipients can be used for LbDDSs, and the selection of the appropriate excipients is a demanding procedure due to *e.g.* insufficient methods currently able to estimate the *in vivo* absorption profile[5, 8]. In this regard, the UNGAP (Understanding Gastrointestinal Absorption-related Processes) European COST Action Network has recently stressed the problems related to a poor comprehension of GI drug absorption, and has highlighted the current approaches and further developments needed in this field[10]. For instance, the *in vitro* intestinal lipolysis model has been developed to investigate the performance of LbDDSs prior to *in vivo* testing[11]. Even though the model provides valuable information on the lipolysis rate of a LbDDS, as well as drug solubilization during lipolysis of a LbDDS, recent studies have shown that the *in vitro* model does to not always predict the *in vivo* performance of LbDDSs in terms of drug absorption[3, 8, 12]. For instance, in the study by Michaelsen *et al.*[12] the amount of fenofibrate found in the aqueous phase after *in vitro* lipolysis of three different

SNEDDSs (*i.e.* $SNEDDS_{75}$, super-SNEDDS $solution_{150}$ and super-SNEDDS $suspension_{150}$) failed to correlate with *in vivo* drug absorption in rats, and it has been proposed that the lack of an absorption step in the *in vitro* lipolysis model could be the reason for the low correlation with *in vivo* data[13]. In parallel, numerous *in vitro* permeability models have been validated to mimic the intestinal mucosa and to assess drug absorption from different drug delivery systems (*e.g*. the Caco-2 model[14]; the PAMPA model[15]; the PVPA model[16]; the Permeapad™[17]; and the AMI system[18]). The PVPA (Phospholipid Vesicle-based Permeation Assay) *in vitro* barriers, composed of liposomes immobilized in and on top of nitrocellulose filters, have been established in the past decade and have proved to simulate the intestinal mucosa[16]. However, all the above-mentioned permeation models were developed without considering the GI digestion affecting LbDDSs. Since neither the *in vitro* lipolysis models nor the *in vitro* permeation models alone are able to provide a full picture of the physiological processes driving GI drug absorption from LbDDSs, they have recently been combined to allow the concomitant study of lipolysis and permeation. For instance, a cell-free artificial membrane, the Permeapad™, has been combined with the *in vitro* intestinal lipolysis model using porcine pancreatin as source of digestive enzymes[6, 13]. Moreover, a cell-based system, the Caco-2 cell model, has been combined with the *in vitro* intestinal lipolysis utilizing immobilized microbial lipase as the digestive enzyme[7, 19, 20]. Several of these combined studies led to improved prediction of *in vivo* absorption data compared to the *in vitro* lipolysis models or *in vitro* permeation models alone[13]. Besides Keemink and Bergstrom[19], where mucin from porcine stomach type III was used as a mean to protect the Caco-2 cell layer, all other models were designed without simulating the mucus layer covering the intestinal wall, thus not fully mimicking the physiological environment of the intestinal mucosa[21]. In fact, the mucus layer is the first barrier that a drug gets in contact with after entering the lumen, and the drug partition between the intestinal luminal fluids, the mucus layer and the intestinal epithelium can affect the extent of drug permeation[21]. Moreover, mucus has shown to affect the absorption of drugs, lipids and

nutrients, and lipid digestion products can conversely modulate the properties of this barrier[22-24]. Therefore, it is of key importance to include the mucus layer in such *in vitro* models, in order to be able to consider its impact on drug absorption. Thus, efforts have been made to simulate the mucus layer covering the GI tract and, as a result of this, an artificial biosimilar mucus (BM) has been developed[25], and proved to resemble both the composition and the rheological properties of porcine intestinal mucus[25, 26].

In light of the importance of including mucus in combined *in vitro* lipolysis-permeation models, as described above, the present study aimed at evaluating if the PVPA *in vitro* permeability model covered with biosimilar mucus would be compatible with a digesting environment. Moreover, the model was tested in terms of its ability to predict the *in vivo* plasma exposure of fenofibrate (poorly water-soluble drug; LogP 5.8[27]) from $SNEDDS_{75}$, super-SNEDDS $solution_{150}$ and super-SNEDDS $suspension_{150}$ previously found by Michaelsen *et al.*[12], and thus lead to *in vivo-in vitro* correlation (IVIVC).

2. Materials and methods

2.1. Materials

Bovine bile, bovine serum albumin (BSA), 4-bromophenyl-boronic acid (BBBA), calcein, cholesterol, fenofibrate, maleic acid, MES hydrate, magnesium sulphate, mucin from porcine stomach type II, pancreatin from porcine pancreas, soybean oil (long-chain (LC) glycerides), tris-(hydroxymethyl)aminomethane (Tris) were products of Sigma Aldrich (St. Luis, MO, USA). Acetonitrile (High-Performance Liquid Chromatography, HPLC, grade), dimethyl sulfoxide (DMSO), ethanol (EtOH; Ph. Eur. Grade), methanol (MeOH; HPLC grade) sodium chloride (NaCl) were purchased from VWR (Herlev, Denmark). Calcium chloride dihydrate, sodium hydroxide were obtained from Merck (Darmstadt, Germany), whereas polysorbate 80 (Tween 80) and polysorbate 20 (Tween 20) were obtained from Fluka Chemie AG (Buchs, Switzerland).

Maisine 35-1 was kindly donated by Gattefossé (St. Priest, France) and Kolliphor RH-40 was kindly received from BASF (Ludwigshafen, Germany). Polyacrylic acid (Carbopol® 974P NF) was purchased from Lubrizol (Brussels, Belgium). E80 lipoid egg-phospholipids (80% phosphatidylcholine) and soy phospholipids (S-PC) were obtained from Lipoid (Ludwigshafen, Germany). All chemicals employed were of analytical grade.

2.2. Methods

2.2.1. Biosimilar mucus preparation

Biosimilar mucus (BM) was prepared following the method described by Boegh *et al.*[25]. Briefly, Carbopol® was dissolved in a hypo-tonic buffer (10 mM MES buffer with 1.0 mM $MgSO_4$ and 1.3 mM $CaCl_2$; pH 6.5) and mucin type II from porcine stomach was added. A lipid mixture was separately prepared in an isotonic buffer (10 mM MES buffer with 1.0 mM $MgSO_4$, 1.3 mM $CaCl_2$ and 137 mM NaCl; pH 6.5) by mixing SPC, cholesterol and polysorbate 80. Finally, BSA and the lipid mixture were added to the Carbopol®-mucin mixture, in order to obtain the final concentrations: Carbopol® (0.9 % w/v), mucin type II from porcine stomach (5 % w/v), S-PC (0.18 % w/v), cholesterol (0.36 % w/v), polysorbate 80 (0.16 % w/v) and BSA (3.1 % w/v). The pH was carefully adjusted to 6.5 and the BM was stored at 4 °C overnight before its use.

2.2.2. PVPA barrier preparation

The PVPA barriers were prepared as previously described by Falavigna *et al.*[28-29]. Briefly, liposomes with two different size distributions (0.4 and 0.8 µm) were obtained using the thin-film hydration technique followed by extrusion. In order to provide immobilization and fusion of the

liposomes, they were centrifuged and freeze-thawed on top of nitrocellulose membrane filters fused to Transwell inserts (surface area 0.33 cm^2) (Corning Inc., New York, USA).

2.2.3. Preparation of SNEDDSs

SNEDDS composed of soybean oil (27.5 % w/w), Maisine 35-1 (27.5 % w/w), Kolliphor RH-40 (35 % w/w) and absolute ethanol (10 % w/w) were prepared following the method previously described by Michaelsen *et al.*[12]. Firstly, soybean oil, Maisine 35-1 and Kolliphor RH-40 were heated at 50 °C, and subsequently Maisine 35-1 and soybean oil were mixed in a 1:1 (w/w) ratio; Kolliphor RH-40 was then added to the mixture, which was left to stir until cooled down to room temperature. Lastly, absolute ethanol was added, and the SNEDDS pre-concentrate was stirred until homogeneity was reached.

Three fenofibrate-loaded SNEDDSs were prepared by adding different amounts of the drug to the pre-concentrate. The equilibrium solubility (S_{eq}) of fenofibrate in the pre-concentrate was previously reported to be 88.5 mg/g[8]. $SNEDDS_{75}$ was prepared by adding drug corresponding to 75 % of the fenofibrate S_{eq} to the pre-concentrate (Table 1) and leaving it to stir at room temperature (23-25 °C) to aid the dissolution process until use. The super-$SNEDDS\ suspension_{150}$ was prepared in the same way as the $SNEDDS_{75}$, but 150% of the S_{eq} was added to the pre-concentrate. The super-$SNEDDS\ solution_{150}$ was prepared by adding drug corresponding to 150 % of the fenofibrate S_{eq} to the pre-concentrate (Table 1), which was then bath-sonicated for 30 minutes, heated for 3 hours at 60 °C, and finally left to cool to 37 °C overnight.

Table 1: Fenofibrate loading and form in the prepared SNEDDSs.

Name	Drug concentration (% of drug S_{eq} in the pre-concentrate)	Drug state
$SNEDDS_{75}$	75	In solution
Super-$SNEDDS\ solution_{150}$	150	In solution
Super-$SNEDDS\ suspension_{150}$	150	In suspension

2.2.4. Solubility studies to select acceptor medium for permeation experiment

The solubility of fenofibrate in different aqueous media was tested in order to select a good acceptor medium for the permeation experiments. The method employed followed the procedure described by Berthelsen *et al.*[30]. Briefly, 10 mg of fenofibrate were suspended in 15 mL of either PBS pH 7.4; Tween 20 5 mg/mL; DMSO 10 mg/mL; DMSO 40 mg/mL; BSA 4% (w/v) or BSA 1% (w/v) (all media were prepared in PBS pH 7.4) and the suspensions were left to rotate at 37 °C for a total of 48 hours. The tubes containing the suspensions were centrifuged after 1, 4, 24 and 48 hours of incubation for 10 minutes at 6500×g, and samples (1 mL) from the supernatant were withdrawn and centrifuged for 10 minutes at 19,000×g. The supernatant was finally diluted with MeOH prior to the quantification of fenofibrate solubilized in the chosen medium. Difference in fenofibrate solubility in one specific medium below 5% between two consequent time points was considered enough to state that the solubility was reached. The quantification of fenofibrate was carried out by HPLC (Dionex UltiMate 3000 pump, ASI 100 automated sample injector, Dionex Ultimate 3000 detector; all from Thermo Fischer, Waltham, MA, USA), using a Phenomenex Kinetix 5u XB-C18 100A column (100 x 4.6 mm; Phenomenex, Torrance, CA, USA). Fenofibrate was detected at a wavelength of 288 nm, with a retention time of approximately 2.5 minutes. The mobile phase was composed of 20% purified water and 80% of MeOH and the flow was set to 1

mL/min. In the case of BSA (1 and 4% w/v) as acceptor medium, acetonitrile was added to the samples in order to precipitate the BSA prior to the quantification *via* HPLC. The solubility in each medium was tested in triplicate (n = 3).

2.2.5. Compatibility of the PVPA barriers with donor and acceptor media

Before the assessment of fenofibrate permeation from SNEDDSs, the permeation of calcein (5.5 mM) was tested to assess the compatibility of the PVPA barriers with the different donor media (Fig. 1B) using PBS pH 7.4 as the acceptor medium. Once the donor media had been evaluated, the compatibility of the PVPA barriers with different acceptor media (see Section 2.2.4) was studied. All experiments were performed at 37 °C. For the experiment being performed in the presence of BM, the mucus layer (50 µL) was carefully pipetted on top of the PVPA barriers and left to incubate for 10 minutes prior to the addition of the donor medium (Fig. 1B). The donor samples (100 µL; Fig. 1B) were directly pipetted on top of the barriers (with or without BM). The barriers were then placed into an acceptor Transwell well containing the acceptor medium (600 µL) and were moved into new wells with the same medium after 2, 4, 5 and 6 hours to uphold sink conditions. At the end of the permeation experiment, calcein P_{app} was calculated and the electrical resistance across the PVPA barriers was measured using a Millicell-ERS volt-ohmmeter (Millicell-ERS, Millipore, USA). The measured electrical resistance was then subtracted with the electrical resistance of the nitrocellulose filter (119 Ohm), and the resulting value was normalized with the surface area of the PVPA barriers (0.33 cm^2). The quantification of calcein was carried out using a Tecan Infinite M200 fluorimeter/spectrophotometer (Salzburg, Austria; Software: Magellan) at excitation wavelength of 485 nm and emission of 520 nm (gain: 70). For each condition tested, 12 PVPA barriers were used (n = 12). Values of calcein P_{app} below $0.06 \cdot 10^{-6}$ cm/s and electrical resistance above 290 Ohm $\cdot$ cm^2 indicate that the integrity of the barriers was maintained[29].

2.2.6. In vitro *lipolysis of fenofibrate-loaded SNEDDSs*

The lipolysis of the SNEDDSs under fasted state conditions using the *in vitro* intestinal lipolysis model was carried out following the method described by Michaelsen *et al.*[12] with minor adjustments. In particular, the SNEDDSs were weighed into a thermostated vessel (37 °C), and subsequently 26 mL of fasted state intestinal medium was added (bile bovine 2.95 mM, calcium chloride 1.40 mM, calcein 5.50 mM, maleic acid 2.00 mM, sodium chloride 146.80 mM, S-PC 0.26 mM, tris 2.00 mM; pH 6.50).

The amount of SNEDDS added into the vessel was adjusted to obtain a final fenofibrate concentration of 480 µg/mL in all experiments, following the procedure described by Michaelsen *et al.*[12]. The pancreatic lipase solution was prepared by mixing the crude lipase extract with 5 mL of intestinal medium in the absence of calcein , centrifuging the mixture for 7 minutes at 6500×g, and collecting the supernatant. Lipolysis was initiated by adding 4 mL of pancreatic lipase solution to the thermostated reaction vessel (final activity of 550 USP/mL). The decrease in pH due to the release of free fatty acids from the digested SNEDDS was countered by the use of an automated pH-stat (Metrohm Titrino 744, Tiamo version 1.3, Herisau, Switzerland) with automated addition of NaOH (0.4 M) in order to keep the pH constant at 6.5. The calcium chloride present in the intestinal medium allowed for a continued lipolysis by removing the free fatty acids by precipitation, and thereby avoiding inhibition of the lipase activity.

Samples (1 mL) were taken from the vessel after dispersion (*i.e.* before lipase addition; 0 minutes) and after 30 minutes of lipolysis, both to be used for the analysis of fenofibrate distribution between the aqueous and pellet phase, and for permeability experiments. Lipolysis in the samples used for the investigation of the fenofibrate distribution was inhibited by the addition of 5 µL BBBA (1 M in MeOH). The inhibited samples (time point 0 and 30 minutes) were centrifuged for

phase separation (19,000×g for 10 minutes), and the concentration of fenofibrate in the aqueous phase was quantified by HPLC after appropriate dilution in MeOH following the method described in Section 2.2.4. To quantify the total amount and determine the recovery of fenofibrate in the lipolysis vessel, samples were taken before centrifugation and analysed by HPLC. The lipolysis was carried out four times for each SNEDDS (n = 4). The permeability samples were directly pipetted (100 µL) on top of the mucus-PVPA barriers to study the permeation of fenofibrate (see Section 2.2.7). The lipolysis of the SNEDDSs was not inhibited for the permeation samples after 30 minutes of lipolysis.

2.2.7. Fenofibrate permeation using the mucus-PVPA model

Once the preferred donor and acceptor media for the permeation experiment had been selected (Section 2.2.5), the permeation of fenofibrate from SNEDDS (*i.e.* $SNEDDS_{75}$, super-SNEDDS $solution_{150}$, super-SNEDDS $suspension_{150}$) was tested using the mucus-PVPA barriers. Calcein was added to all donor media, in order to enable an in-line assessment of the mucus-PVPA barrier integrity (data not shown). As described above (Section 2.2.5), BM was pipetted (50 µL) on top of the PVPA barriers 10 minutes prior to the addition of the donor sample (100 µL). The donor sample was either obtained after dispersion of SNEDDSs in the intestinal medium (*i.e.* sample before lipolysis; time point 0 minutes), or after 30 minutes of lipolysis (*i.e.* digesting SNEDDSs in intestinal medium; no lipolysis inhibition). The barriers were then placed into an acceptor Transwell well containing the acceptor medium (600 µL) and were moved into new wells with the same medium after 2, 4, 5 and 6 hours to uphold sink conditions. The electrical resistance across the PVPA barriers was measured after 6 hours to test if the integrity of the barriers was maintained, as discussed above (Section 2.2.5). The quantification of calcein and fenofibrate in the acceptor compartment was carried out using a Tecan Infinite M200 fluorimeter/spectrophotometer (Salzburg, Austria; Software: Magellan) at excitation wavelength

of 485 nm and emission of 520 nm (gain: 70) for calcein and 288 nm for fenofibrate. For each condition tested, six PVPA barriers were used (n = 6).

2.2.8. Calculations

The apparent permeability (P_{app}) of calcein was calculated using the following equation:

$$P_{app}\left(\frac{cm}{s}\right) = \frac{dQ}{dt} * \frac{1}{A * Cd}$$

Where *dQ/dt* expresses the flux at the steady state (nmol/s), *A* is the surface area of the PVPA barriers (0.33 cm^2) and C_d the initial fenofibrate/calcein concentration in the donor compartment (nmol/mL).

The area under the curve (AUC) was calculated using GraphPad Prism 7.03 (GraphPad Software, San Diego, CA, USA), which employed a linear trapezoidal model from t = 0 to t = 6 h.

2.2.9. Statistical analysis

GraphPad Prism 7.03 was employed for the statistical analysis of the presented results (GraphPad Software, San Diego, CA, USA). The data was analysed using one-way ANOVA followed by Šidák *post hoc* test to detect significant differences ($p < 0.05$) when comparing three or more sets of data. If a comparison between two sets of data was made, student t-test was employed ($p < 0.05$).

3. Results and discussion

In this study, the development and validation of the *in vitro* lipolysis – mucus-PVPA permeation model was carried out. Biosimilar mucus (BM) was added on top of the PVPA barriers, leading to a better simulation of the intestinal mucosa, which also contains a mucus layer.

The integrity of the PVPA barriers was evaluated in the presence of BM, simulated intestinal medium, undigested and digesting SNEDDSs. The lipolysis of fenofibrate-loaded SNEDDSs was studied using the *in vitro* intestinal lipolysis model, followed by the drug permeation assessment using the mucus-PVPA barriers. Finally, the correlation of *in vitro* lipolysis and lipolysis-permeation data with *in vivo* plasma data of fenofibrate in rats was determined. The type of IVIVC assessed in this study can be referred to as a Level D correlation, and it is considered a qualitative correlation which can be used in the development of new formulations[31].

3.1. Lipolysis-permeation model setup

3.1.1. Donor medium selection

The compatibility of the PVPA barriers, with and without mucus, with the donor medium compositions in Fig. 1B, using PBS pH 7.4 as acceptor medium, was evaluated by assessing the permeation of the hydrophilic marker calcein, and the electrical resistance across the barriers at the end of the permeation assay (see Section 2.2.5).

As it can be observed in Fig. 1, the PVPA barriers were able to maintain their functionality in all the tested donor media in the presence of BM. In the absence of BM, the medium with undigested $SNEDDS_{75}$ (Fig. 1, Setup 5) led to barrier impairment; calcein P_{app} was $0.29 \cdot 10^{-6}$ cm/s and the electrical resistance was 208 Ohm $\cdot$ cm^2, which were both values outside the limits set for intact barriers (*i.e.* calcein P_{app} above $0.06 \cdot 10^{-6}$ cm/s and electrical resistance below 290 Ohm $\cdot$ cm^2 indicate loss of barrier integrity[28]). However, the digested $SNEDDS_{75}$ in the donor compartment showed to be compatible with the barrier also in the absence of mucus (Fig. 1, Setup 7). The

difference in barrier compatibility between the undigested and digested SNEDDS$_{75}$ might be due to the colloidal structures that are generated during the lipolysis of SNEDDSs. SNEDDS$_{75}$ before lipolysis display a very distinct structure characterized by nano-emulsion droplets, while during lipolysis their lipid fractions result in the formation of different colloidal structures, such as vesicles and micelles, composed of both lipolysis products and components present in the simulated intestinal medium[12].

BM, fasted state simulated intestinal medium, undigested SNEDDS$_{75}$ (in the presence of BM) and digested SNEDDS$_{75}$ (both with uninhibited and inhibited pancreatin) were compatible with the barriers (Fig. 1). As the presence of BM maintained barrier integrity with undigested SNEDDS$_{75}$ (Fig. 1, Setup 6), BM was applied on top of the barriers during the assessment of the permeation of fenofibrate from SNEDDSs before and after *in vitro* lipolysis.

A

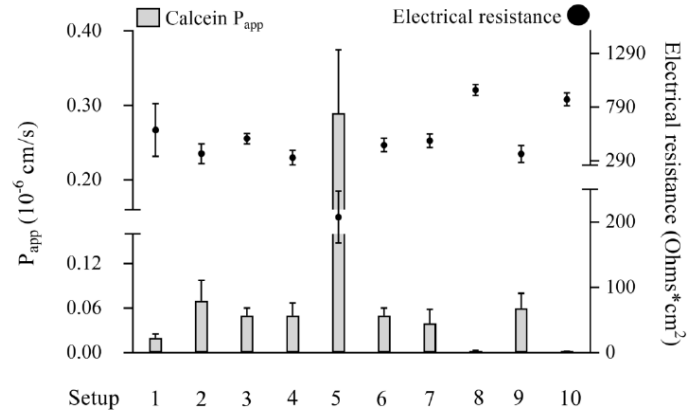

B

Setup	Donor medium	BM	Sample added to donor medium
1	PBS Control	✗	Calcein
2	PBS Control	✓	Calcein
3	Intestinal medium	✗	Calcein
4	Intestinal medium	✓	Calcein
5	Intestinal medium	✗	Calcein + SNEDDS$_{75}$
6	Intestinal medium	✓	Calcein + SNEDDS$_{75}$
7	Intestinal medium	✗	Calcein + digesting SNEDDS$_{75}$
8	Intestinal medium	✓	Calcein + digesting SNEDDS$_{75}$
9	Intestinal medium	✗	Calcein + digested SNEDDS$_{75}$+ BBBA
10	Intestinal medium	✓	Calcein + digested SNEDDS$_{75}$+ BBBA

Fig. 1: A) PVPA barrier integrity expressed as apparent permeability (P_{app}) of calcein (5.5 mM) and electrical resistance across the PVPA barriers with different setups (Mean ± SD; n = 12). B)

Setups tested in terms of PVPA barrier compatibility with and without BM. PBS pH 7.4 was used as the acceptor medium.

3.1.2. Acceptor medium selection

The solubility of fenofibrate was determined in the acceptor medium for the permeation study described in Section 2.2.4. Higher solubility of the lipophilic drug in the acceptor compartment of the PVPA model would enable a larger amount of drug to permeate, thereby easing the quantification of the amount of permeated drug. As can be observed in Table 2, the highest solubility of fenofibrate was in Tween 20 5 mg/mL and BSA 4% w/v. Moreover, DMSO significantly increased the solubility of fenofibrate at a concentration of 40 mg/mL, but not at 10 mg/mL, when compared to PBS pH 7.4 (Table 2).

Table 2: Equilibrium solubility of fenofibrate in different aqueous media prepared in PBS pH 7.4 (Mean ± SD; n = 3). *Statistically significant difference in fenofibrate equilibrium solubility compared to PBS pH 7.4 ($p < 0.05$).

Acceptor medium	Equilibrium solubility (nmol/mL)
PBS pH 7.4	0.48 ± 0.03
DMSO 10 mg/mL	0.59 ± 0.08
DMSO 40 mg/mL	0.82 ± 0.01*
BSA 1% w/v	14.19 ± 0.13*
BSA 4% w/v	58.02 ± 0.49*
Tween 20 5 mg/mL	116.71 ± 5.73*

Only DMSO (1-40 mg/mL) has previously been investigated regarding its compatibility with the PVPA barriers[32], and showed not to impair the integrity of the barriers up to a concentration of 40 mg/mL. Thus, to select the best acceptor medium, the functionality of the barriers in the presence

of each acceptor medium was investigated before performing permeation experiments, while using calcein solution (in PBS pH 6.5; 5.5 mM) on the donor side. As can be seen in Fig. 2 the barriers maintained their integrity in the presence of PBS pH 7.4 and DMSO (10 and 40 mg/mL). In contrast, BSA (1 and 4% w/v) and Tween 20 5 mg/mL caused barrier impairment, as demonstrated by an increased calcein P_{app} and decreased electrical resistance. Based on the effect on PVPA barrier integrity and the solubility of fenofibrate, DMSO 40 mg/mL was chosen as the acceptor medium in the fenofibrate permeation studies.

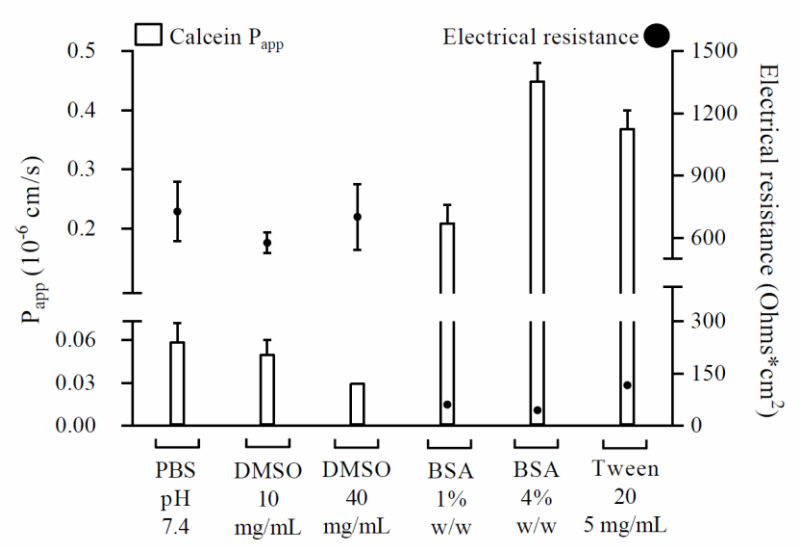

Fig. 2: PVPA barrier integrity expressed as apparent permeability (P_{app}) of calcein (5.5 mM) and electrical resistance across the barriers with different media in the acceptor compartment, and calcein 5.5 mM in the donor compartment (in PBS pH 6.5). (Mean ± SD; n = 12).

3.2. In vitro *lipolysis* of fenofibrate-loaded SNEDDSs

Three SNEDDSs ($SNEDDS_{75}$, super-$SNEDDS\ solution_{150}$ and super-$SNEDDS\ suspension_{150}$) were analysed in terms of their capability of solubilizing fenofibrate after 30 minutes of *in vitro* lipolysis. Fig. 3 depicts the distribution of fenofibrate in the aqueous and the pellet phase before (0 min) and after (30 min) lipolysis. For $SNEDDS_{75}$, little to no precipitation was observed both

before (0 min) and after (30 min) lipolysis, while for the super-SNEDDS solution$_{150}$, precipitation of fenofibrate was observed at the start of lipolysis and after 30 minutes. In the case of the super-SNEDDS suspension$_{150}$, the presence of drug precipite was pronounced both after dispersion (0 min) and after lipolysis (30 min), and a significant increase over time ($p < 0.05$) was observed when comparing the amount of precipitate before and after lipolysis (Fig. 3). The differences between the SNEDDSs can be due to that twice as much SNEDDS$_{75}$ was added, compared to the super-SNEDDS solution$_{150}$ and the super-SNEDDS suspension$_{150}$, in order to keep the fenofibrate concentration constant in the lipolysis vessel. This lower amount of lipid caused a decrease in drug solubilization and an increase in drug precipitation.

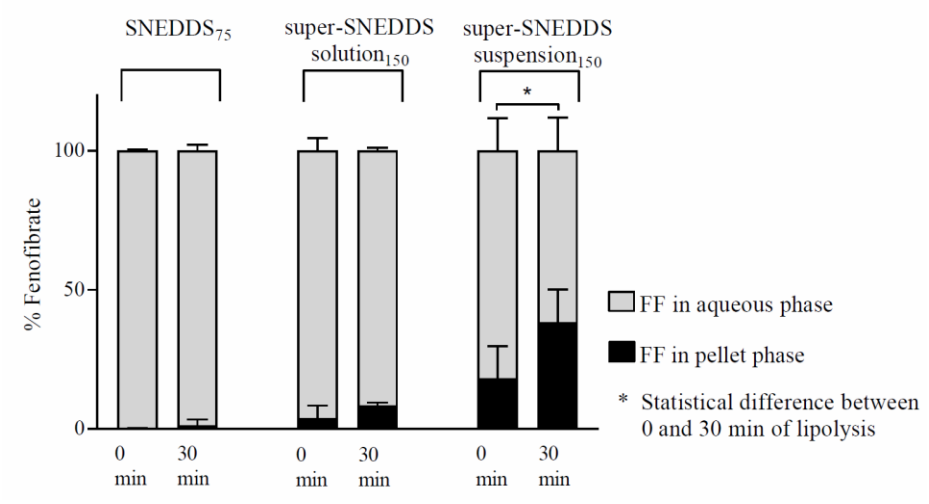

Fig. 3: Relative amount of fenofibrate present in the aqueous phase (*grey*) and pellet phase (*black*) during *in vitro* intestinal lipolysis of SNEDDS$_{75}$, super-SNEDDS solution$_{150}$ and super-SNEDDS suspension$_{150}$. (Mean ± SD; n = 4). * Statistical difference between the percentages of fenofibrate in solution after 0 minutes compared to 30 minutes of lipolysis.

When comparing the two super-SNEDDSs, containing the same amount of lipid vehicle, the presence of precipitated fenofibrate was more pronounced for the super-SNEDDS suspension$_{150}$

(Fig. 3). This is due to the nature of the super-SNEDDS suspension$_{150}$ where the drug is only partially dissolved, whereas the drug is completely dissolved in the super-SNEDDS solution$_{150}$.

Michaelsen *et al.*[12], studied the same fenofibrate-containing SNEDDSs, and the impact of fenofibrate load and SNEDDSs lipolysis on drug solubilization and absorption was evaluated *via* an *in vivo* pharmacokinetic study in rats and *in vitro* lipolysis. The results depicted in Fig. 3 are in accordance with the *in vitro* lipolysis data obtained by Michaelsen *et al.*[12]. Even though the ranking in terms of drug precipitation of the three SNEDDSs was the same as the findings in the present study, the percentage of drug precipitated during lipolysis was higher in the results presented by Michaelsen *et al.*[12]. The difference in drug precipitation between the two studies can be explained by the different experimental setups of the *in vitro* lipolysis applied in the two studies: in the present study, calcium was added to the simulated intestinal medium prior to lipolysis (initial/bolus addition of calcium) to simplify the experimental setup, whereas in the study by Michaelsen *et al.*[12] calcium was continuously added during lipolysis to control the rate of lipolysis (dynamic addition of calcium). It has previously been demonstrated that initial and continuous addition of calcium can lead to differences in terms of drug precipitation during lipolysis of LbDDSs, and that the calcium concentration can also have an effect on the extent of lipolysis[33].

3.3. In vivo *absorption*-in vitro *lipolysis correlation*

In the study by Michaelsen *et al.*[12], the super-SNEDDS solution$_{150}$ had a superior *in vivo* performance after oral dosing to rats (*i.e.* higher $AUC_{0\text{-}30h,\ in\ vivo}$ and C_{max}) compared to SNEDDS$_{75}$ and super-SNEDDS suspension$_{150}$ (Table 3). This was not correlating with the observed drug solubilisation during *in vitro* lipolysis, where SNEDDS$_{75}$ led to a higher drug solubilization. Thus, Michaelsen *et al.*[12] were not able to find a correlation between the *in vivo* absorption and the drug solubilization during *in vitro* lipolysis.

Table 3: Area under the curve (AUC) resulting from fenofibrate absorption during *in vivo* studies in rats ([*12], $AUC_{0\text{-}30h,\ in\ vivo}$), % of fenofibrate found in the aqueous phase after 30 min of *in vitro* lipolysis, and AUC resulting from the mass transfer of fenofibrate permeated across the mucus-PVPA barriers ($AUC_{0\text{-}6h,\ perm}$) before (0 min) and after (30 min) *in vitro* lipolysis from super-SNEDDS $solution_{150}$, $SNEDDS_{75}$ and super-SNEDDS $suspension_{150}$. Values labelled with the same letter are significantly different. (Mean ± SEM; n = 6).

	Super-SNEDDS $solution_{150}$	$SNEDDS_{75}$	Super-SNEDDS $suspension_{150}$
$AUC_{0\text{-}30h,\ in\ vivo}$ (µg·h/mL) *in vivo* rats*	148.0 ± 47.5[a, b]	88.3 ± 20.9[a]	58.1 ± 16.9[b]
Fenofibrate (%) in the aqueous phase after 30 min of *in vitro* lipolysis	91.7 ± 1.11	98.6 ± 2.1	61.8 ± 11.9
$AUC_{0\text{-}6h,\ perm}$ (nmol·h) *in vitro* mucus-PVPA: fenofibrate permeation before lipolysis	17.0 ± 1.6[c]	14.0 ± 1.2	9.9 ± 2.2[c]
$AUC_{0\text{-}6h,\ perm}$ (nmol·h) *in vitro* mucus-PVPA: fenofibrate permeation after 30 min *in vitro* lipolysis	17.0 ± 0.8[d, e]	12.0 ± 1.0[d]	8.7 ± 1.1[e]

In accordance with the findings from Michaelsen *et al.*[12], the present study did not find a correlation between the drug solubilized during *in vitro* lipolysis (Section 3.2) and the *in vivo* plasma data (R^2 = 0.397; Fig. 4, Table 3), highlighting the fact that *in vitro* solubilization alone cannot predict the *in vivo* absorption of fenofibrate from the SNEDDS analyzed in this study. Even though it is generally assumed that the SNEDDS able to maintain the most drug in solution during lipolysis leads to the highest bioavailability[34], it should be noted that the amount of fenofibrate in the aqueous phase during *in vitro* lipolysis is in a dynamic equilibrium between free drug and drug solubilized in vesicles and other colloidal structures resulting from the lipolysis products (*e.g.* free

fatty acids and monoglycerides) and their interaction with bile salts and phospholipid in the medium[13]. Only the free drug is available for absorption, and therefore it is of interest to quantify this, by adding a permeation step to the *in vitro* lipolysis.

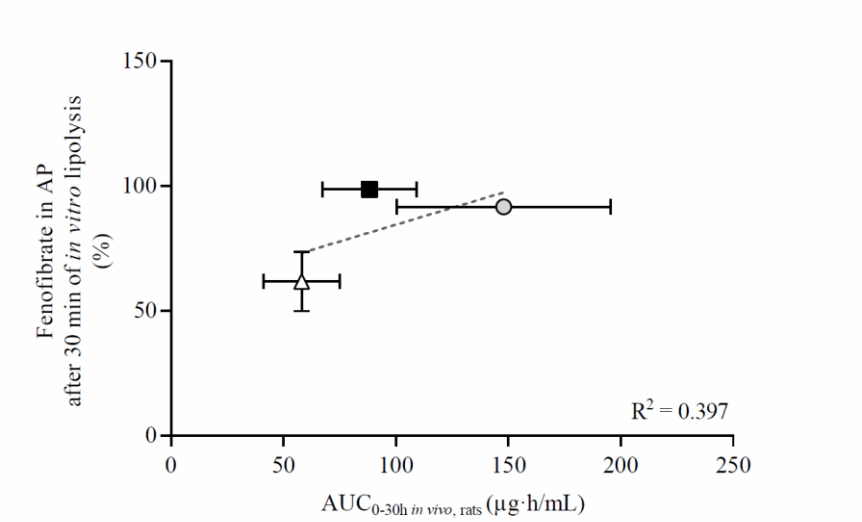

Fig. 4: Fenofibrate (%) found in the aqueous phase (AP) after 30 min of *in vitro* lipolysis as a function of the $AUC_{0\text{-}30h,\ in\ vivo}$ from the plasma curve after oral dosing in rats (Michaelsen et al., 2019[12]) of super-SNEDDS $solution_{150}$ (*grey circle*), $SNEDDS_{75}$ (*black square*) and super-SNEDDS $suspension_{150}$ (*white triangle*).

3.4. In vitro *permeation*

The permeation of fenofibrate across the mucus-PVPA barriers following administration of three different SNEDDSs was evaluated before (0 min) and after (30 min) *in vitro* lipolysis. This allowed the investigation of whether fenofibrate permeation was influenced by i) SNEDDSs composition and ii) lipolysis of the SNEDDSs. The in-line assessment of the mucus-PVPA barrier integrity carried out by measuring the permeation of calcein confirmed the correct functionality of the mucus-PVPA barriers (data not shown), and confirmed that the componenets present in the donor compartment of the permeation barriers did not affect the mucus-PVPA barriers integrity.

As can be observed from Fig. 5, both before and after lipolysis, the super-SNEDDS solution$_{150}$ allowed the highest permeation of fenofibrate, followed by the SNEDDS$_{75}$ and the super-SNEDDS suspension$_{150}$. Even though the ranking of the three SNEDDSs was the same before (Fig. 5A) and after lipolysis (Fig. 5B), differences in the permeation profiles in the two conditions led to differences in $AUC_{0\text{-}6h,\ perm}$ (Table 3). The $AUC_{0\text{-}6h,\ perm}$ for the undigested super-SNEDDS solution$_{150}$ was significantly higher than for the super-SNEDDS suspension$_{150,}$ but not the SNEDDS$_{75}$. After 30 minutes of *in vitro* lipolysis, the $AUC_{0\text{-}6h,\ perm}$ for the super-SNEDDS solution$_{150}$ was significantly higher than the $AUC_{0\text{-}6h,\ perm}$ for both the super-SNEDDS suspension$_{150}$ and the SNEDDS$_{75}$ (Table 3). This is in accordance with the *in vivo* data presented by Michaelsen *et al.*[12] where the ranking of the *in vivo* $AUC_{0\text{-}30h,\ in\ vivo}$ was: super-SNEDDS solution$_{150}$ > SNEDDS$_{75}$ > super-SNEDDS suspension$_{150}$ (Table 3). The difference between the $AUC_{0\text{-}6h,\ perm}$ before and after lipolysis can be explained by a change in drug concentration in the aqueous phase upon lipolysis. The nanoemulsion droplets of SNEDDS formed after dispersion in the intestinal medium (*i.e.* before *in vitro* lipolysis) can have a different impact on drug solubilization compared to the colloidal structures formed during lipolysis. This will especially impact the equilibrium between the amount of drug free in solution and the one associated with colloidal structures, and thus the amount of drug available for permeation across the PVPA barriers.

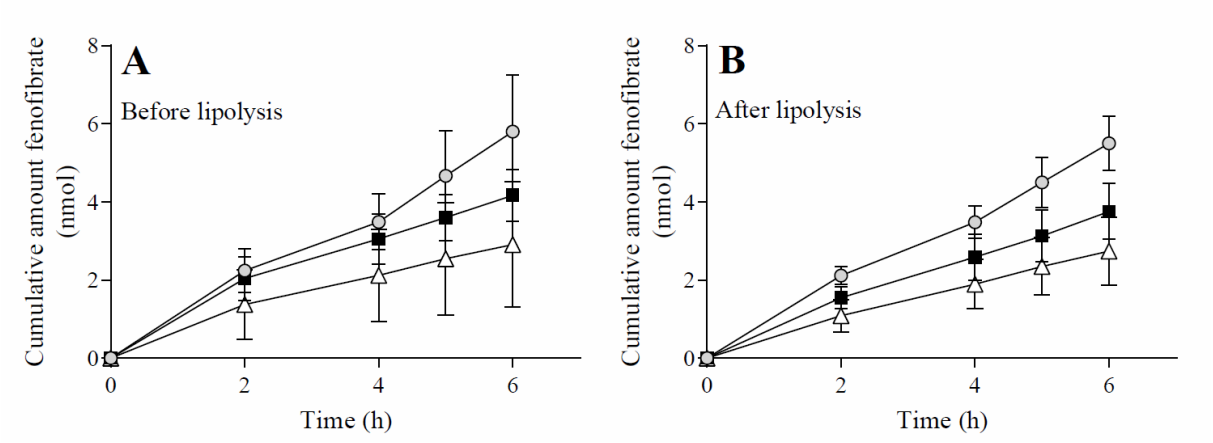

Fig. 5: Cumulative amount of fenofibrate permeated across the mucus-PVPA barriers from super-SNEDDS solution$_{150}$ (*grey circle*), SNEDDS$_{75}$ (*black square*) and super-SNEDDS suspension$_{150}$ (*white triangle*) A) before (0 min) and B) after (30 min) lipolysis. (Mean ± SD; n = 6).

The results discussed thus far demonstrate that, even though the total drug concentration in the donor compartment was the same (480 µg/mL) for all the analysed SNEDDSs, the amount of fenofibrate permeating through the barriers was affected by the SNEDDS in the donor compartment. Moreover, even though the *in vitro* lipolysis showed that the SNEDDS$_{75}$ resulted in the highest amount of drug solubilized in the aqueous phase (Fig. 3), the super-SNEDDS solution$_{150}$ exhibited the highest permeation (Fig. 5). Thomas *et al.*[35] have demonstrated that drug precipitation following lipolysis of super-SNEDDS solutions does not necessarily translate to lower *in vivo* drug absorption. The difference in drug permeation between the super-SNEDDS solution$_{150}$ and SNEDDS$_{75}$ can be due to the partitioning of the drug between being free in solution and in the colloidal structures, formed upon dispersion/lipolysis of the SNEDDS on top of the permeation barriers. For SNEDDS$_{75}$, the lipid content is higher, and more drug can be associated to the colloidal structures, thus not being able to permeate. In contrast, for super-SNEDDS solution$_{150}$, the lower lipid content can lead to a higher amount of drug being free in solution, and thus able to permeate through the mucus-PVPA barriers, as demonstrated in Fig. 5.

462 *3.5.* In vivo *absorption*-in vitro *permeation correlation*

463 To assess the correlation between *in vitro* and *in vivo* data, the *in vitro* $AUC_{0\text{-}6h,\ perm}$ from the
464 fenofibrate permeation was depicted as a function of the *in vivo* $AUC_{0\text{-}30h,\ in\ vivo}$ (Table 3[12]) in Fig.
465 6. The correlation of the permeation data after 30 minutes of *in vitro* lipolysis was better (Fig. 6B,
466 $R^2 = 0.9952$) compared to the permeation of fenofibrate from undigested SNEDDSs (Fig. 6A, R^2
467 = 0.9255), highlighting the positive impact of the presence of lipolysis on the IVIVC. Comparing
468 these findings to Fig. 4, it is clear that for the investigated SNEDDSs, the amount of drug
469 solubilised during *in vitro* lipolysis studies alone cannot predict the *in vivo* absorption of
470 fenofibrate, while an additional permeation step can enable a prediction of the performance of
471 SNEDDS *in vivo*.

472

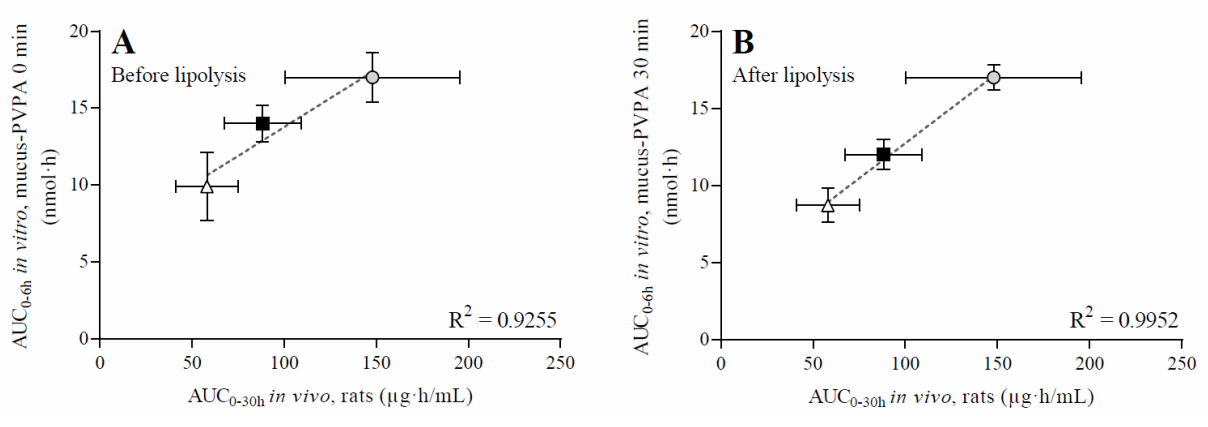

473

474 **Fig. 6**: *In-vivo-in-vitro* correlation (IVIVC) of *in vivo* plasma exposure (Michaelsen et al., 2019[12])
475 and *in vitro* fenofibrate permeation across the mucus-PVPA barriers A) before (0 min) and B) after
476 (30 min) lipolysis from super-SNEDDS solution$_{150}$ (*grey circle*), SNEDDS$_{75}$ (*black square*) and
477 super-SNEDDS suspension$_{150}$ (*white triangle*).

478

479 In the present study, the presence of the BM layer on top of the absorptive PVPA barriers permitted
480 the development of a permeation model able to withstand a digesting environment (Fig. 1).

Moreover, the addition of BM on top of the PVPA barriers allowed for a better simulation of the intestinal mucosa, and possibly contributed to the estimation of the *in vivo* performance of the SNEDDSs tested by Michaelsen *et al.*[12]. As all the *in vitro* fenofibrate permeation experiments were performed in the presence of mucus, the comparison in terms of drug permeation between the presence and absence of the mucus layer could not be assessed. The hydrophilic mucus barrier in the mucus-PVPA model has previously shown to affect drug permeation depending on the physicochemical properties of the investigated drug, drug formulation and the simulated physiological conditions[28, 29, 36], and it is thus regarded as an essential part of the artificial absorption barrier. The presence of mucus is also important as it has been shown that SNEDDSs can rapidly permeate across this layer thanks to the low interaction of their hydrophobic surface with the hydrophilic regions of mucus and thanks to their low droplet size, consequently enabling higher drug absorption[37-38]. Thus, the inclusion of mucus on top of an *in vitro* permeation membrane is crucial to simulate the environment that SNEDDSs would be presented to *in vivo,* and allows these drug delivery systems to explicate the positive effect on drug absorption related to their high mucus permeation.

4. Conclusion

In the present study, the *in vitro* lipolysis – mucus-PVPA permeation model was developed. The model allowed the combination of the assessment of drug distribution during lipolysis for fenofibrate-loaded SNEDDSs typical of the *in vitro* intestinal lipolysis model with the quantification of the fenofibrate permeation through an artificial membrane mimicking the intestinal epithelium (*i.e.* mucus-PVPA barrier). The barriers used in this work were more stable when lined with a mucus layer, thus being able to closely mimic the physiology of the intestinal mucosa and to improve the relevance of the model for oral absorption studies. The investigated SNEDDSs had different abilities to keep fenofibrate solubilized in the aqueous phase during *in*

vitro lipolysis, and led to different drug permeation profiles. No correlation was found between already published *in vivo* absorption and drug solubilisation during *in vitro* lipolysis ($R^2 < 0.4$), whereas a satisfactory correlation was found between the same *in vivo* data with *in vitro* permeation data both before and after *in vitro* lipolysis ($R^2 > 0.9$), highlighting the importance of the permeation step following lipolysis in the prediction of *in vivo* drug absorption. The combination of *in vitro* lipolysis with *in vitro* permeation led to a better correlation ($R^2 = 0.9952$) compared to absence of lipolysis ($R^2 = 0.9255$). However, the satisfactory correlation in the absence of lipolysis suggests that this step might not be necessary. In order to validate this statement, further studies with other types of SNEDDSs need to be carried out.

By applying the *in vitro* lipolysis – mucus-PVPA permeation model, it was possible to mimic physiological processes (*i.e.* lipolysis and permeation) and to correlate the amount of fenofibrate permeated *in vitro* with the AUC after oral dosing of the applied SNEDDSs in rats.

Acknowledgments

The authors acknowledge UiT The Arctic University of Norway for funding PhD student Margherita Falavigna. The authors thank Lipoid GmbH (Ludwigshafen, Germany) for the donation of phospholipids. The contributions from NordicPOP (supported by NordForsk for the Nordic University Hub project number: 85352), and COST Action UNGAP (supported by the European Cooperation in Science and Technology; project number: 16205) are greatly appreciated.

Conflict of interest

The authors confirm no conflicts of interest.

References

[1] Porter CJH, Trevaskis NL, Charman WN. Lipids and lipid-based formulations: optimizing the oral delivery of lipophilic drugs. Nat. Rev. Drug Discov. 2007; 6 (3): 231–248. https://doi.org/10.1038/nrd2197

[2] Gao P, Morozowich W. Development of supersaturatable self-emulsifying drug delivery system formulations for improving the oral absorption of poorly soluble drugs. Expert opinion on drug delivery 2006; 3 (1): 97–110. https://doi.org/10.1517/17425247.3.1.97

[3] Siqueira SDVS, Müllertz A, Gräeser K, Kasten G, Mu H, Rades T. Influence of drug load and physical form of cinnarizine in new SNEDDS dosing regimens: in vivo and in vitro evaluations. AAPS J. 2017;19 (2): 587-594. https://doi.org/10.1208/s12248-016-0038-4

[4] Trevaskis NL, Charman WN, Porter CJH. Lipid-based delivery systems and intestinal lymphatic drug transport: a mechanistic update. Adv. Drug Deliv. Rev. 2008; 60 (6): 702–716. https://doi.org/10.1016/j.addr.2007.09.007

[5] Feeney OM, Crum MF, McEvoy CL, Trevaskis NL,Williams HD, Pouton CW, Charman WN, Bergström CAS, Porter CJH. 50 years of oral lipid-based formulations: Provenance, progress and future perspectives. Adv. Drug Deliv. Rev. 2016; 101: 167-194. https://doi.org/10.1016/j.addr.2016.04.007

[6] Bibi HA, Holm R, Bauer-Brandl A. Simultaneous lipolysis/permeation in vitro model, for the estimation of bioavailability of lipid based drug delivery systems. Eur. J. Pharm. Biopharm. 2017; 117: 300–307. https://doi.org/10.1016/j.ejpb.2017.05.001

[7] Keemink J, Mårtensson E, Bergström CAS. Lipolysis-Permeation setup for simultaneous study of digestion and absorption in vitro. Mol. Pharm. 2019; 16: 921-930. https://doi.org/10.1021/acs.molpharmaceut.8b00811

[8] Thomas N, Richter K, Pedersen TB, Holm R, Müllertz A, Rades T. In vitro lipolysis data does not adequately predict the in vivo performance of lipid-based drug delivery systems containing fenofibrate. AAPS J. 2014; 16 (3): 539-549. https://doi.org/10.1208/s12248-014-9589-4

[9] Savla R, Browne J, Plassat V, Wasan KM, Wasan EK. Review and analysis of FDA approved drugs using lipid-based formulations. Drug Develop. Ind. Pharm. 2017; 43: 1743-1758. https://doi.org/10.1080/03639045.2017.1342654

[10] Boyd BJ, Bergström CAS, Vinarov Z, Kuentz M, Brouwere J, Augustijns P, Brandl M, Bernkop-Schnürch A, Shrestha N, Préath V, Müllertz A, Bauer-Brandl A, Jannin V. Successful oral delivery of poorly water-soluble drugs both depends on the intraluminal behaviour of drugs and of appropriate advanced drug delivery systems. Eur. J. Pharm. Sci. 2019; 137: 104967. https://doi.org/10.1016/j.ejps.2019.104967

[11] Zangenberg NH, Müllertz A, Kristensen HG, Hovgaard L. A dynamic in vitro lipolysis model I. Controlling the rate of lipolysis by continuous addition of calcium. Eur. J. Pharm. Sci. 2001; 14: 115-122. https://doi.org/10.1016/s0928-0987(01)00169-5

[12] Michaelsen MH, Siqueira Jørgensen SD, Abdi IM, Wasan KM, Rades T, Müllertz A. Fenofibrate oral absorption from SNEDDS and super-SNEDDS is not significantly affected by lipase inhibition in rats. Eur. J. Pharm. Biopharm. 2019; 142: 258-264. https://doi.org/10.1016/j.ejpb.2019.07.002

[13] Berthelsen R, Klitgaard M, Rades T, Müllertz A. In vitro digestion models to evaluate lipid based drug delivery systems; present status and current trends. Adv. Drug Deliv. Rev. 2019; 142: 35-49. https://doi.org/10.1016/j.addr.2019.06.010

[14] Artursson P, Palm K, Luthman K. Caco-2 monolayers in experimental and theoretical predictions of drug transport. Adv. Drug Deliv. Rev. 2001; 46: 27–43. https://doi.org/10.1016/s0169-409x(00)00128-9

[15] Kansy M, Senner F, Gubernator K. Physicochemical high throughput screening: parallel artificial membrane permeation assay in the description of passive absorption processes. J. Med. Chem.1998; 41: 1007–1010. https://doi.org/10.1021/jm970530e

[16] Flaten GE, Dhanikula AB, Luthman K, Brandl M. Drug permeability across a phospholipid vesicle barrier: a novel approach for studying passive diffusion. Eur. J. Pharm. Sci. 2006; 27: 80–90. https://doi.org/10.1016/j.ejps.2005.08.007

[17] di Cagno M, Bibi HA, Bauer-Brandl A. New biomimetic Permeapad™ for efficient investigation of passive permeability of drugs. Eur. J. Pharm. Sci. 2015; 73: 29–34. https://doi.org/10.1016/j.ejps.2015.03.019

[18] Berben P, Brouwers J, Augustijns P. Assessment of passive intestinal permeability using an artificial membrane insert system. J. Pharm. Sci. 2018; 107: 250–256. https://doi.org/10.1016/j.xphs.2017.08.002

[19] Keemink J, Bergstrom CAS. Caco-2 cell conditions enabling studies of drug absorption from digestible lipid-based formulations. Pharm. Res. 2018; 35: 74. https://doi.org/10.1007/s11095-017-2327-8

[20] Alskär LC, Parrow A, Keemink J, Johansson P, Abrahamsson B, Bergström CAS. Effect of lipids on absorption of carvedilol in dogs: Is coadministration of lipids as efficient as a lipid-based formulation? J. Control. Release 2019; 304: 90-100. https://doi.org/10.1016/j.jconrel.2019.04.038

[21] Lechanteur A, das Neves J, Sarmento B. The role of mucus in cell-based models used to screen mucosal drug delivery. Adv. Drug Deliv. Rev. 2018; 124: 50-63. https://doi.org/10.1016/j.addr.2017.07.019

[22] Miyazaki K, Kishimoto H, Muratani M, Kobayashi H, Shirasaka Y, Inoue K. Mucins are Involved in the Intestinal Permeation of Lipophilic Drugs in the Proximal Region of Rat Small Intestine. Pharm. Res. 2019; 36 (162): 1-11. https://doi.org/10.1007/s11095-019-2701-9

[23] Rezhdo O, Speciner L, Carrier R. Lipid-associated oral delivery: Mechanisms and analysis of oral absorption enhancement. J. Control. Release 2016; 240: 544-560. https://doi.org/10.1016/j.jconrel.2016.07.050

[24] Yildiz HM, Speciner L, Ozdemir C, Cohen DE, Carrier RL. Food-associated stimuli enhance barrier properties of gastrointestinal mucus. Biomaterials 2015; 54: 1-8. https://doi.org/10.1016/j.biomaterials.2015.02.118

[25] Boegh M, Baldursdóttir SG, Müllertz A, Nielsen HM. Property profiling of biosimilar mucus in a novel mucus-containing in vitro model for assessment of intestinal drug absorption. Eur. J. Pharm. Biopharm. 2014; 87: 227-235. https://doi.org/10.1016/j.ejpb.2014.01.001

[26] Boegh M, Garcia-Diaz M, Müllertz A, Nielsen HM. Steric and interactive barrier properties of intestinal mucus elucidated by particle diffusion and peptide permeation. Eur. J. Pharm. Biopharm. 2015; 95: 136-143. https://doi.org/10.1016/j.ejpb.2015.01.014

[27] Roese E, Bunjes H. Drug release studies from lipid nanoparticles in physiological media by a new DSC method. J. Control. Release 2017; 256: 92-100. https://doi.org/10.1016/j.jconrel.2017.04.032

[28] Falavigna M, Klitgaard M, Brase C, Ternullo S, Skalko-Basnet N, Flaten GE. Mucus-PVPA (mucus phospholipid vesicle-based permeation assay): an artificial permeability tool for drug screening and formulation development. Int. J. Pharm. 2018; 537: 213–222. https://doi.org/10.1016/j.ijpharm.2017.12.038

[29] Falavigna M, Klitgaard M, Steene E, Flaten GE. Mimicking regional and fasted/fed state conditions in the intestine with the mucus-PVPA in vitro model: The impact of pH and simulated intestinal fluids on drug permeability. Eur. J. Pharm. Sci. 2019; 132: 44-54. https://doi.org/10.1016/j.ejps.2019.02.035

[30] Berthelsen R, Sjögren E, Jacobsen J, Kristensen J, Holm R, Abrahamsson B, Müllertz A. Combining in vitro and in silico methods for better prediction of surfactant effects on the absorption of poorly water soluble drugs – a fenofibrate case example. Int. J. Pharm. 2014; 473: 356–365. https://doi.org/10.1016/j.ijpharm.2014.06.060

[31] Schen JS, Burgess DJ. In Vitro-In Vivo Correlation for Complex Non-Oral Drug Products: Where Do We Stand? J. Control. Release 2015; 219: 644-651. https://doi.org/10.1016/j.jconrel.2015.09.052

[32] Flaten GE, Luthman K, Vasskog T, Brandl M. Drug permeability across a phospholipid vesicle-based barrier: 4. The effect of tensides, co-solvent and pH changes on barrier integrity and on drug permeability. Eur. J. Pharm. Sci. 2008; 34: 173–180. https://doi.org/10.1016/j.ejps.2008.04.001

[33] Sassene P, Kleberg K, Williams HD, Bakala-N'Goma JC, Carrière F, Calderone M, Jannin V, Igonin A, Partheil A, Marchaud D, Jule E, Vertommen J, Maio M, Blundell R, Benameur H, Porter CJH, Pouton CW, Müllertz A. Toward the establishment of standardized in vitro tests for lipid-based formulations, Part 6: effects of varying pancreatin and calcium levels. AAPS J. 2014; 16 (6): 1344-1356. https://doi.org/10.1208/s12248-014-9672-x

[34] Dahan A, Hoffman A. Use of a dynamic in vitro lipolysis model to rationalize oral formulation development for poor water soluble drugs: correlation with in vivo data and the relationship to intra-enterocyte processes in rats. Pharm. Res. 2006; 23 (9): 2165-2174. https://doi.org/10.1007/s11095-006-9054-x

[35] Thomas N, Holm R, Müllertz A, Rades T. In vitro and in vivo performance of novel supersaturated self-nanoemulsifying drug delivery systems (super-SNEDDS). J. Control. Release 2012; 160: 25-32. https://doi.org/10.1016/j.jconrel.2012.02.027

679

680 [36] Falavigna M, Stein PC, Flaten GE, Pio di Cagno M. Impact of Mucin on Drug Diffusion:
681 Development of a Straightforward in Vitro Method for the Determination of Drug Diffusivity in
682 the Presence of Mucin. Pharmaceutics 2020; 12 (168): 1-13.
683 https://doi.org/10.3390/pharmaceutics12020168

684

685 [37] Abdulkarim M, Sharma PK, Gumbleton M. Self-emulsifying drug delivery system: Mucus
686 permeation and innovative quantification technologies. Adv. Drug Deliv. Rev. 2019; 142: 62-74.
687 https://doi.org/10.1016/j.addr.2019.04.001

688

689 [38] Leal J, Smyth HDC, Ghosh D. Physicochemical properties of mucus and their impact on
690 transmucosal drug delivery. Int. J. Pharm. 2017; 532: 555-572.
691 https://doi.org/10.1016/j.ijpharm.2017.09.018